The ribonuclease domain function is dispensable for SLFN11 to mediate cell fate decision during replication stress response

Fei Qi[1,2,3], Erin Alvi[2], Minori Ogawa[2], Junya Kobayashi[1,3], Anfeng Mu[2,4]*, Minoru Takata[1,2,4]*

[1]Department of Interdisciplinary Environmental Sciences, Graduate School of Human and Environmental Sciences, Kyoto University, Kyoto, Japan
[2]Laboratory of DNA Damage Signaling, Department of Late Effects Studies, and [3]Laboratory of Cancer Cell Biology, Department of Genome Dynamics, Radiation Biology Center, Graduate School of Biostudies, Kyoto University, Kyoto, Japan.
[4]Multilayer Network Research Unit, Research Coordination Alliance, Kyoto University, Kyoto, Japan

*Corresponding authors: Phone +81-75-753-7563, Fax +81-75-753-7564, Email mu.anfeng.7x@kyoto-u.ac.jp or takata.minoru.8s@kyoto-u.ac.jp

Current address (E.A.): Laboratory of Biochemical Cell Dynamics, Institute for Integrated Cell-Material Sciences (WPI-iCeMS), Graduate School of Biostudies, Kyoto University, Kyoto, Japan.
Current address (J.K.): Department of Radiological Sciences, School of Health Sciences at Narita, International University of Health and Welfare, Kozunomori 4-3, Narita-shi 286-8686, Japan

Abstract

The *SLFN11* gene participates in cell fate decision following cancer chemotherapy and encodes the N-terminal ribonuclease (RNase) domain and the C-terminal helicase/ATPase domain. How these domains contribute to the chemotherapeutic response remains controversial. Here, we expressed SLFN11 containing mutations in two critical residues required for RNase activity in *SLFN11*$^{-/-}$ cells. We found that this mutant was still able to suppress DNA damage tolerance, destabilized the stalled replication forks, and perturbed recruitment of the fork protector RAD51. In contrast, we confirmed that the helicase domain was essential to accelerate fork degradation. The fork degradation by the RNase mutant was dependent on both DNA2 and Mre11 nuclease, but not on Mre11's novel interactor FXR1. Collectively, these results supported the view that the RNase domain function is dispensable for SLFN11 to mediate cell fate decision during replication stress response.

Key words: DNA damage, SLFN11, replication stress, stalled fork degradation, DNA helicase, ATR

Introduction

The *Schalfen (SLFN)* gene family was identified in developing mice thymocytes and the name ("sleep" in German) was coined since they generally prevent cell growth when expressed(Schwarz et al., 1998). The *SLFN* family is mostly mammalian-specific and has undergone rapid diversification probably due to their involvement in the immune response. SLFN11, a long-form member of the SLFN gene family, participates in various biological processes such as anti-viral defense or replication stress response (Bustos et al., 2009; Jo & Pommier, 2022; F. Liu et al., 2018; Schwarz et al., 1998). In many human cancer and cancer-derived cell lines, the *SLFN11* gene is often silenced and not expressed. Thus, *SLFN11* might function as a tumor suppressor (Jo et al., 2021). Loss of SLFN11 rendered cancer cells generally more tolerant to replication stress and DNA damage during anti-cancer drug treatments (Zoppoli et al., 2012). Hence, *SLFN11* is critical for cell fate decision following cancer chemotherapy and is now proposed to be a potential biomarker to predict clinical outcome following chemotherapy (Sousa et al., 2015; Zhang et al., 2021). However, how the expression of *SLFN11* mechanistically affects cancer development and facilitates cell death after DNA damage remains to be established. The long-form SLFNs (including SLFN11) harbor two functional modules: the N-terminal core domain containing ribonuclease features and the C-terminal helicase/ATPase domain

(Jo & Pommier, 2022). To understand how SLFN11 can affect the biological behavior of cancer cells, it might be important to elucidate the role of these domains and whether they are functionally inter-connected.

The C-terminal helicase domain has been reported to mediate cell fate decisions in response to DNA damage and replication stress. It has been well established that stalled replication forks are reversed by the actions of fork remodeling enzymes such as SMARCAL1, resulting in a 4-way junction structure which is subjected to digestion by nucleases like DNA2 and MRE11. Fork degradation must be tightly regulated for resumption of replication, and hence, cell survival (Berti et al., 2020). We have previously implicated the role of *SLFN11* in accelerating stalled fork degradation, by preventing recruitment of the fork protector RAD51 (Okamoto et al., 2021)We proposed that this fork instability may be the basis for enhanced DNA damage sensitivity by SLFN11. Several additional mechanisms have been suggested to enhance DNA damage sensitivity: *SLFN11* suppresses DNA repair activity due to homologous recombination and affects checkpoint maintenance (Mu et al., 2016), blocks replication fork progression (Murai et al., 2018), or promotes the degradation of the replication factor CDT1 (Jo et al., 2021).

In contrast, it was also shown that SLFN11 RNase activity downregulates protein levels of ATR kinase, which is critical for the cellular response to DNA damage and

replication stress, thereby decreasing viability following DNA damage (Li et al., 2018). ATR accumulates at the stalled forks by binding to RPA via its subunit ATRIP and is activated through binding with the ATR-activating domain of TopBP1 or ETAA1 (Saldivar et al., 2017). ATR phosphorylates its substrates, which are crucial for downstream checkpoint and replication stress responses. Li et al. reported that the codon usage of ATR is distinct and its translation depends on a specific subset of tRNAs, which are the target of SLFN11 RNase activity (Li et al., 2018). Consistent with this idea, it is well established that the RNase domain of SLFN family members is involved in translational regulation by cleaving tRNA/rRNA as an endonuclease and exerting anti-HIV activity, which is present in hSLFN13 (Yang et al., 2018) as well as in hSLFN11 (Li et al., 2012; Metzner, Huber, et al., 2022; Metzner, Wenzl, et al., 2022).

It is difficult to reconcile these two lines of evidence each depending on the N-terminal RNase domain and C-terminal helicase domain, respectively. In this study, we planned to obtain insights into the role of the SLFN11 RNase domain in the replication stress response. Based on the structural and biochemical data in the literature (Li et al., 2012; Yang et al., 2018), we made a SLFN11 RNase domain mutant, in which two functionally critical residues were both changed to alanine, and expressed this mutant in *SLFN11*$^{-/-}$ HAP1 cells. Our analysis revealed that the RNase domain mutant can suppress

cell survival following hydroxyurea (HU) treatment and destabilize stalled replication forks similarly to wild-type SLFN11. Nucleases (i.e., DNA2 and MRE11) were similarly promoted for digestion by the RNase domain mutant. Not unexpectedly, a novel MRE11 interactor FXR1 (FMR1 autosomal homolog 1) which we have previously identified (Qi et al., 2020), was dispensable. In contrast, SLFN11 with the mutated ATPase/helicase domain could not facilitate HU-induced fork degradation. Furthermore, we observed that the exogenous expression of neither wild type nor RNase-mutant SLFN11 has an impact on protein levels of ATR kinase in HAP1 cells.

Results

SLFN11 enhances cellular sensitivity to DNA-damaging reagents independent of its RNase domain.

Previous works by us and others indicated that *SLFN11* enhances DNA damage sensitivity via its C-terminal helicase domain. However, the SLFN11 protein also has an N-terminal core domain which acts as a ribonuclease (RNase) for a specific subset of tRNA/rRNA (Metzner, Huber, et al., 2022; Yang et al., 2018) and is engaged in translation control of ATR kinase (Li et al., 2018). Therefore, we decided to investigate whether the RNase domain of SLFN11 is responsible for affecting DNA damage sensitivity or not. To this

aim, we introduced two inactivating mutations on the critical residues in the RNase domain in the N-terminal SLFN11 core domain (Figure 1A and B) and tested whether the expression of SLFN11 with the RNase domain mutations could restore the phenotype caused by the loss of human *SLFN11* in human HAP1 cells (Okamoto et al., 2021). These two residues are very well conserved among SLFN family members and are shown to be critical for tRNA cleavage by SLFN13 or SLFN11 (Figure 1A and B) (Metzner, Wenzl, et al., 2022; Yang et al., 2018). Because we found the exogenous expression of *SLFN11* is difficult to achieve and tends to be lost over a short period, the introduction of *SLFN11* was carried out with lentivirus vectors encoding DOX-inducible GFP-tagged wild-type SLFN11(+SLFN11 WT) or RNase domain mutant SLFN11(+SLFN11 RNase mut) into *SLFN11*$^{-/-}$ HAP1 cells and GFP-tagged SLFN11 expressing cells can be visible with microscope. The expression of SLFN11 in the clones selected by hygromycin was confirmed following 48 h induction of DOX treatment with immunoblotting using an anti-SLFN11 antibody (Figure 1C), though RNase domain mutation decreased the expression levels compared to WT SLFN11.

We firstly assessed the proliferation of cells expressing wild-type SLFN11 or the RNase domain mutant. It has been reported that *SLFN11*-depleted cells proliferated significantly faster than wild-type HAP1 cells, and the exogenous *SLFN11* expression

decreased cell growth rate (Okamoto et al., 2021). Indeed, we observed that the *SLFN11*$^{-/-}$ HAP1 cells grew faster than the wild-type HAP1 cells (Figure 1D), and expression of both wild-type and the RNase domain mutant similarly decreased growth rate (Figure 1D).

Hydroxyurea (HU), a ribonucleotide reductase inhibitor, causes depletion of the deoxynucleotide pool in the cell, thereby inducing replication stress and stalled replication forks. We investigated whether SLFN11 with mutations in the RNase domain affects cellular sensitivity to HU. Consistent with the previous findings (Okamoto et al., 2021), we observed that DOX-induced wild-type SLFN11 expression in HAP1 cells partially restored cellular sensitivity to HU (Figure 1E). Furthermore, expression of the RNase domain mutant SLFN11 also increased cellular sensitivity to HU (Figure 1E), suggesting that the RNase domain of SLFN11 is dispensable for its function in reversing cellular sensitivity to DNA-damaging reagents.

To exclude effects on SLFN11 function by GFP-tagging, a parallel lentiviral construct in which SLFN11 was fused with FLAG tag was introduced into *SLFN11*$^{-/-}$ HAP1 cells. The expression of SLFN11s were observed in both FLAG-tagged wild-type and RNase domain mutant SLFN11 in *SLFN11*$^{-/-}$ HAP1 cells (Supplementary figure 1A). Not surprisingly, similarly to the GFP-tagged SLFN11 expressions, we observed that HU

sensitivity was partially restored by FLAG-tagged WT SLFN11 as well as RNase domain mutant (Supplementary figure 1B).

SLFN11 accelerates replication fork degradation in a manner independent of its RNase domain

We have previously reported that *SLFN11* prevents the recruitment of the fork protector RAD51 to nascent DNA sites during replication stress, thereby accelerating stalled fork degradation (Okamoto et al., 2021). To test whether the SLFN11 RNase domain plays a crucial role in accelerating HU-induced fork degradation, we utilized the DNA fiber assay. Progressing replication forks in HAP1 cells were pulse-labeled with thymidine analogs, 5-iodo-2'-deoxyuridine (IdU) followed by 5-chloro-2'-deoxyuridine (CldU) then exposed to 4 mM HU for 5 h to stall progressing replication forks (Figure 2A, upper). The tract length of CldU-labeled DNA was assessed as an index of nascent DNA degradation in a blinded manner. Consistent with the previous findings (Okamoto et al., 2021), we observed that the length of CldU tracts in wild-type HAP1 cells were shortened (degraded) following HU treatment, while there were no significant changes in the CldU tract lengths of *SLFN11*$^{-/-}$ HAP1 cells with and without HU treatment (Figure 2A and B). We further carried out DNA fiber assays in *SLFN11*$^{-/-}$ HAP1 cells complemented with

wild-type SLFN11, RNase domain mutant or the helicase domain mutant. We found that re-expression of wild-type, as well as the RNase domain mutant, significantly shortened CldU tract length during HU treatment (Figure 2A and B). However, the CldU tract length was not altered with or without HU treatment in cells in which the Helicase/ATPase domain mutant SLFN11 was re-expressed (Supplementary figure 2). These results suggested that the helicase function, but not RNase activity, was required for accelerating nascent replication fork degradation.

SLFN11 prevents RPA and RAD51 recruitment to DNA damage sites in a manner independent of its RNase domain

Since we previously reported that *SLFN11* may enhance replication fork degradation by impeding RAD51 recruitment to the stalled replication fork (Okamoto et al., 2021). To examine whether the RNase activity of SLFN11 have any role in RAD51 recruitment, we tested RAD51 and RPA foci formation in *SLFN11*$^{-/-}$ HAP1 cells expressing the RNase domain mutant following HU treatment with immunofluorescence. We confirmed that both RPA and RAD51 foci formation were enhanced in *SLFN11*$^{-/-}$ HAP1cells after treatment with HU compared to WT HAP1 cells (Figure 3) as we reported before (Okamoto et al., 2021). In contrast, both RPA and RAD51 foci formation were decreased

expression of FLAG-tagged wild-type SLFN11 as well as the RNase mutant SLFN11 (Figure 3). These results suggested that *SLFN11* prevents Rad51 loading onto nascent DNA sites thereby accelerating replication fork degradation in a manner independent of its RNase domain.

Expression of SLFN11 carrying a mutated RNase domain enhances degradation of replication forks in a manner dependent on nuclease DNA2 or MRE11

It has been reported that nucleases such as DNA2 and MRE11 participate in digestion of nascent DNA of stalled replication forks during HU treatment (Rickman & Smogorzewska, 2019). Our previous research indicated that *SLFN11* promotes fork degradation in combination with nucleases including DNA2 or MRE11 (Okamoto et al., 2021). We performed a DNA fiber assay to test whether the RNase domain mutation could affect this process. We confirmed that siRNA targeting DNA2 or MRE11 in both wild-type and *SLFN11*$^{-/-}$ HAP1 cells successfully decreased DNA2 expression levels with western blotting (Figure 4A). We then observed that DNA2 knockdown could increase the CldU tract length in wild-type as well as *SLFN11*$^{-/-}$ HAP1 cells re-expressing wild-type SLFN11 post-HU treatment, but could not further elongate the tract length in *SLFN11*$^{-/-}$ HAP1 cells (Figure 4B). As expected, DNA2 knockdown also prevented

shortening of the tract length in *SLFN11*$^{-/-}$ HAP1 cells expressing the RNase mutant SLFN11 (Figure 4B). Furthermore, MRE11 knockdown showed a similar tendency to DNA2 knockdown in HAP1 cells with each genotype (Figure 4B), indicating that both DNA2 and MRE11 are crucial for fork degradation that is promoted by *SLFN11*. Our previous research identified FXR1(FMR1 autosomal homolog 1), an RNA-binding protein, as a novel MRE11 interactor (Qi et al., 2020). It could bind with MRE11 in mitochondria and contributes to cellular defense against mitochondrial reactive oxidative stress. To test whether FXR1 acts in fork degradation, we performed the DNA fiber assay in *FXR1*-depleted HAP1 cells (Figure 4B). However, we observed that the FXR1 knockdown did not significantly affect fork degradation in any of the genotypes tested (Figure 4B). Taken together, these results suggest that *SLFN11* promotes replication fork degradation in a manner dependent on nuclease DNA2 and MRE11, but not FXR1. Our data further indicate that the RNase domain of SLFN11 is dispensable for the acceleration of stalled fork degradation.

Expression of *SLFN11* did not affect ATR kinase protein levels in replication stress response.

It has been previously described that *SLFN11* inhibits translation of ATR kinase through cleavage of specific types of tRNA during the DNA damage response, due to the distinct

codon usage in ATR (Li et al., 2018). Because this report is apparently at odds with our current observation, we decided to investigate whether SLFN11 expression could affect the expression and function of ATR kinase in response to HU-induced replication stress in HAP1 cells. RT-PCR analysis did not reveal decreased ATR mRNA levels in either expression of wild-type SLFN11 or RNase mutant SLFN11(Figure 5A). Western blot analysis showed that levels of ATR protein expression was not affected after HU treatment in both *SLFN11*$^{-/-}$ cells and wild type cells. Furthermore, expression of wild-type SLFN11 and RNase mutant SLFN11 also show no effects on ATR protein expression levels. The phosphorylation levels of CHK1 on S345, which is known to be phosphorylated by ATR, also did not show difference after HU treatment between cells expressing wild-type and RNase mutant SLFN11. The Ser4/Ser8 phosphorylation of RPA, which is mediated by DNA-PKcs (S. Liu et al., 2012), was enhanced following HU treatment in parental *SLFN11*$^{-/-}$ and complemented cells with SLFN11 wild-type or RNase mutant compared to WT HAP1 cells (Figure 5B and Supplementary figure 3A). The reason for this difference were unclear but could be due to clonal variation. In addition, the exogenous expression of wild type SLFN11 in K562 cells, which originally do not express SLFN11, did not show any impacts on ATR expression (Supplementary figure 3B). Taken together,

irrespective of the SLFN11 RNase domain mutations, we could not observe that the expression of SLFN11 reduces ATR kinase expression.

Discussion

There are two conflicting views in the literature on the mechanisms of SLFN11-mediated enhanced DNA damage sensitivity, which seem difficult to reconcile. While the C-terminal helicase domain of SLFN11 is proposed to modulate DNA metabolism such as DNA repair (Mu et al., 2016)or replication (Jo et al., 2021; Murai et al., 2018), the N-terminal RNase domain is suggested to downregulate translation of critical replication stress kinase ATR, leading to loss of checkpoint response (Li et al., 2018). In this study, we created the RNase domain mutant and expressed it in *SLFN11*$^{-/-}$ cells. We provide lines of evidence that indicate the RNase domain is dispensable for replication stress response and degradation of stalled replication forks. In contrast, the equivalent RNase domain mutants in SLFN13 or SLFN11 are shown to be deficient in tRNA cleavage (Metzner, Wenzl, et al., 2022; Yang et al., 2018). Consistently, the effect of the knockdown of nucleases DNA2 and MRE11 on fork degradation were similar in both cells expressing wild-type and the RNase deficient mutant SLFN11. We also confirmed that the fork degradation during HU-induced replication stress was promoted in a manner dependent

on the ATPase/helicase domain. Thus, we conclude that the SLFN11 function during replication stress response is mediated via the helicase domain but not through the RNase domain in HAP1 cells.

Consistent with the above conclusion, we also observed that there was no significant reduction in ATR protein expression in response to replication stress in WT HAP1 cells as well as in *SLFN11*$^{-/-}$ cells transduced with either wild-type or RNase mutant SLFN11. The ATR levels in SLFN11-deficient K562 cells could not be affected by the exogenous expression of SLFN11. These observations were contrast to the conclusion described by Li et al. (Li et al., 2018), which implicates SLFN11-mediated tRNA cleavage in ATR downregulation with its RNase activity thereby promote cellular sensitivity to DNA-damaging agent. The reason for this discrepancy is unclear and could be due to the use of different cell lines and methods. More experiments are needed to resolve this contradiction.

Experimental Procedures

Cell culture

HAP1 cells were derived from the human haploid chronic myelogenous leukemia (CML) cell line KBM-7 and cultured in IMDM (Nacalai Tesque) supplemented with 10% Fetal

Bovine Serum (FBS). Cells were treated with Hydroxyurea (HU) (Millipore Sigma) at the indicated concentrations. HEK293T cells were cultured in DMEM-high glucose (Nacalai Tesque) supplemented with 10% FBS. K562 cells with or without SLFN11 expression [12] were kindly provided by Dr. Junko Murai (Ehime University Medical School) and maintained in RPMI1640 medium (Nacalai Tesque) supplemented with 10% FBS.

Antibodies

The following antibodies were obtained from commercial sources: mouse monoclonal anti-SLFN11 (E4; 374339; Santa Cruz Biotechnology); rabbit polyclonal anti-DNA2 (ab96488; Abcam); rabbit polyclonal anti–phospho-CHK1 (Ser345; 133D3, 2348; Cell Signaling); rabbit polyclonal anti–phospho-CHK1 (Ser345; 2341; Cell Signaling); rabbit polyclonal anti-phospho-ATR (T1989; 58014; Cell Signaling); rabbit polyclonal anti-ATR (ab2905; Abcam); mouse monoclonal anti-MRE11(GTX70212; Genetex); rabbit polyclonal anti-FXR1 (A303-892A; Bethyl); mouse monoclonal anti-5-bromo-29-deoxyuridine (BrdU) (anti-IdU; 347580; BD Biosciences); rat polyclonal anti-BrdU (anti-CldU; ab6326; Abcam); mouse monoclonal anti-tubulin (T5168; Millipore Sigma); HRP-conjugated anti-mouse, or anti-rabbit IgG antibodies (GE Healthcare) and Alexa Fluor

594-conjugated anti-mouse IgG and Alexa Fluor 488-conjugated anti-rat IgG antibodies (Molecular Probes).

Generation of the *SLFN11* mutants

The wild-type *SLFN11* coding sequence cloned in pENTR plasmid is mutated by inverse PCR (forward 5'-CGTCTCAGTTAGTAGCGTTTAAACAGTTCT-3', reverse 5'-GCTACTAACTGAGACGCAGGAAAAGGCAGG-3'; Invitrogen), and confirmed by Sanger sequencing. The mutated *SLFN11* was transferred to the lentivirus plasmid CSIV (RIKEN) by the Gateway system using Clonase II (Invitrogen). Construction of the ATPase dead mutant (K605M/D668A) was described previously (Mu et al., 2016; Okamoto et al., 2021).

Lentivirus transduction in *SLFN11*$^{-/-}$ HAP1 cell line

The generation of *SLFN11*$^{-/-}$ HAP1 cells was described previously[10]. To express wild-type and mutant *SLFN11* under doxycycline-controlled transcriptional activation, lentivirus transduction was utilized. HEK293T cells were transfected with CSIV plasmid, together with packaging constructs pCAG-HIVgp, and pCMV-VSV-G-RSV-Rev using the Lipofectamine3000 reagent (Invitrogen) according to the manufacturer's instructions.

SLFN11$^{-/-}$ HAP1 cells were infected with viral supernatants and stable pools were selected with 400 μg/mL hygromycin (Nacalai Tesque). Single clones were isolated and verified by western blotting. *SLFN11* expression was induced by treatment with 2 μg/ml doxycycline (DOX) for 48 h.

Small interfering RNA (siRNA) transfection

Transfection and co-transfection were carried out using Lipofectamine RNAi Max (Invitrogen). The individual siRNA duplexes used were as follows: siDNA2 (5'-CAUCCAAUAUUUUCCCGUA-3'; MilliporeSigma) siMRE11 (5'-GAUGAGAACUCUUGGUUUATT-3'; B-Bridge International Inc); siFXR1 (5'-GGUUCGAGUGAGAAUUGAATT -3'; Qiagen Co); and Luciferase Control (siLuc; 5'-UCGAAGUAUUCCGCGUACGTT-3'; MilliporeSigma).

Cell growth assay and cytotoxicity assay

For cell growth assay, HAP1 cells (1×10^5) were seeded into 6 cm dishes at day 0 and counted every 24 h. For cytotoxicity assays, HAP1 cells (2.5×10^3) were plated in a 96-well plate in a quadruplicate for each condition. After 48 h of DOX pre-treatment (*SLFN11*-transduced cells), the indicated concentration of HU was added to the wells and

incubated for additional 72 h. Cell viability was measured using a Cell Counting Reagent SF (Nacalai Tesque). Absorbance at 450 nm was measured with a Multilabel Reader (PerkinElmer).

Immunoblotting

After drug treatment, cells were harvested and lysed with 1X SDS buffer (containing 2-mercaptoethanol) at a final concentration of $5x10^6$ cells/ml. Samples were separated by sodium dodecyl sulfate-polyacrylamide gel electrophoresis (SDS-PAGE) or Extra PAGE One Precast Gel (Nacalai Tesque) SDS-PAGE gel. Electrophoresed proteins were transferred to a polyvinylidene difluoride (PVDF) membrane and reacted with indicated antibodies. After the membrane was incubated with ECL plus chemiluminescence system (GE Healthcare) for 5 min at room temperature, the target proteins were visualized with Image Quant LAS 4000mini (Cytiva).

Reverse-transcription PCR assay

Total RNA was extracted using RNeasy Plus Mini Kit (QIAGEN, # 74134). PrimeScript™ RT reagent kit with gDNA Eraser (TaKaRa) was used for the first-strand cDNA synthesis with 1 μg total RNA. PCR amplification was carried out using KOD-FX

polymerase (TOYOBO) with gene-specific primers: (hATR, forward 5'-GCTGGTTTGAGACCTATTCTGAC-3', reverse 5'-CATATATGGAGTCCAACCAAGATAC-3'; hGAPDH, forward 5'-ACCCAGAAGACTGTGGATGG-3', reverse 5'-TTCTAGACGGCAGGTCAGGT-3'; Invitrogen). These experiments were carried out according to the manufacturer's instructions with a lower cycle number to avoid the plateau effects.

Immunohistochemistry

HAP1 cells (5×10^3) were plated in 96-well plates (PerkinElmer). Cells were stimulated with or without HU and fixed with 3% paraformaldehyde/2% sucrose in PBS for 30 min and then permeabilized with 0.1% Triton X-100/PBS for another 30 min. After blocking with 2% BSA/PBS, cells were incubated with indicating primary antibodies diluted in 2% BSA diluted with PBS, followed by incubated with secondary antibodies. Nuclei were counterstained with DAPI (Sigma-Aldrich). The quantification of foci was using an INCellAnalyzer2000 instrument (Cytiva).

DNA fiber assay

The DNA fiber assay was carried out essentially as described before [10] in a blinded

manner. Cells were firstly labeled with 25 μM IdU for 30 min, then washed with PBS twice, and the second labeling was done with 250 μM CldU for another 30 min. Subsequently, cells were treated with or without 4 mM HU for 5 h. Cells were collected and suspended in 70% ethanol at a final concentration of 5 x 10^5 cells/ml. Fibers labeled with IdU (red) then CldU (green) were measured using the Leica DM5500B microscope and Leica Application Suite X (LAS X) software. The degradation of nascent DNA (second tract length) of each sample was analyzed with Prism software (Graphpad).

ACKNOWLEDGEMENT

We would like to thank Dr.Yusuke Okamoto for discussions; Dr. Junko Murai for providing K562 cells expressing SLFN11; the late Dr. Hiroyuki Miyoshi and RIKEN BRC for the Lentivirus system; Ms. Masami Tanaka, Mayu Yamabe, Sumiko Matsui, Xuye Wang, and Lin Liu for technical and secretarial assistance. **Author contributions:** A.M., J.K., and M.T. designed the study. Erin Alvi compared the protein sequences and cloned the cDNAs. Fei Qi carried out DNA fiber analysis with the help of Minori Ogawa. Fei Qi, Anfeng Mu, and Minoru Takata wrote the manuscript, and Erin Alvi provided English editing.

FUNDING

A.M. is supported by the Kyoto University Research Coordination Alliance. This work is partly supported by the KAKENHI Kiban B (Grant# 20H03450 to M.T.), KAKENHI Kiban C (Grant# 20K12162 to J.K.), Takeda Science Foundation (to A.M.), and JSPS Core-to-Core Program (Grant# JPJSCCA20200009).

DATA AVAILABILITY

The data that support the findings of this study are available on request from the corresponding author.

CONFLICT OF INTEREST

The authors declare no competing financial interests

References

Berti, M., Cortez, D., & Lopes, M. (2020). The plasticity of DNA replication forks in response to clinically relevant genotoxic stress. *Nature Reviews Molecular Cell Biology*, *21*(10), 633–651. https://doi.org/10.1038/s41580-020-0257-5

Bustos, O., Naik, S., Ayers, G., Casola, C., Perez-Lamigueiro, M. A., Chippindale, P. T., Pritham, E. J., & de la Casa-Esperón, E. (2009). Evolution of the Schlafen genes, a gene family associated with embryonic lethality, meiotic drive, immune processes and orthopoxvirus virulence. *Gene*, *447*(1), 1–11. https://doi.org/10.1016/j.gene.2009.07.006

Jo, U., Murai, Y., Chakka, S., Chen, L., Cheng, K., Murai, J., Saha, L. K., Miller Jenkins, L. M., & Pommier, Y. (2021). SLFN11 promotes CDT1 degradation by CUL4 in response to replicative DNA damage, while its absence leads to synthetic lethality with ATR/CHK1 inhibitors. *Proceedings of the National Academy of Sciences of the United States of America*, *118*(6), 1–12. https://doi.org/10.1073/pnas.2015654118

Jo, U., & Pommier, Y. (2022). Structural, molecular, and functional insights into Schlafen proteins. *Experimental and Molecular Medicine*, *54*(6), 730–738. https://doi.org/10.1038/s12276-022-00794-0

Li, M., Kao, E., Gao, X., Sandig, H., Limmer, K., Pavon-Eternod, M., Jones, T. E., Landry, S., Pan, T., Weitzman, M. D., & David, M. (2012). Codon-usage-based inhibition of

HIV protein synthesis by human schlafen 11. *Nature*, *491*(7422), 125–128. https://doi.org/10.1038/nature11433

Li, M., Kao, E., Malone, D., Gao, X., Wang, J. Y. J., & David, M. (2018). DNA damage-induced cell death relies on SLFN11-dependent cleavage of distinct type II tRNAs. *Nature Structural & Molecular Biology*, *25*(11), 1047–1058. https://doi.org/10.1038/s41594-018-0142-5

Liu, F., Zhou, P., Wang, Q., Zhang, M., & Li, D. (2018). The Schlafen family: complex roles in different cell types and virus replication. In *Cell Biology International* (Vol. 42, Issue 1, pp. 2–8). Wiley-Blackwell Publishing Ltd. https://doi.org/10.1002/cbin.10778

Liu, S., Opiyo, S. O., Manthey, K., Glanzer, J. G., Ashley, A. K., Amerin, C., Troksa, K., Shrivastav, M., Nickoloff, J. A., & Oakley, G. G. (2012). Distinct roles for DNA-PK, ATM and ATR in RPA phosphorylation and checkpoint activation in response to replication stress. *Nucleic Acids Research*, *40*(21), 10780–10794. https://doi.org/10.1093/nar/gks849

Metzner, F. J., Huber, E., Hopfner, K. P., & Lammens, K. (2022). Structural and biochemical characterization of human Schlafen 5. *Nucleic Acids Research*, *50*(2), 1147–1161. https://doi.org/10.1093/nar/gkab1278

Metzner, F. J., Wenzl, S. J., Kugler, M., Krebs, S., Hopfner, K.-P., & Lammens, K. (2022). Mechanistic understanding of human SLFN11. *Nature Communications*, *13*(1), 5464. https://doi.org/10.1038/s41467-022-33123-0

Mu, Y., Lou, J., Srivastava, M., Zhao, B., Feng, X., Liu, T., Chen, J., & Huang, J. (2016). SLFN 11 inhibits checkpoint maintenance and homologous recombination repair . *EMBO Reports*, *17*(1), 94–109. https://doi.org/10.15252/embr.201540964

Murai, J., Tang, S. W., Leo, E., Baechler, S. A., Redon, C. E., Zhang, H., Al Abo, M., Rajapakse, V. N., Nakamura, E., Jenkins, L. M. M., Aladjem, M. I., & Pommier, Y. (2018). SLFN11 Blocks Stressed Replication Forks Independently of ATR. *Molecular Cell*, *69*(3), 371-384.e6. https://doi.org/10.1016/j.molcel.2018.01.012

Okamoto, Y., Abe, M., Mu, A., Tempaku, Y., Rogers, C. B., Mochizuki, A. L., Katsuki, Y., Kanemaki, M. T., Takaori-Kondo, A., Sobeck, A., Bielinsky, A.-K., & Takata, M. (2021). *SLFN11 promotes stalled fork degradation that underlies the phenotype in Fanconi anemia cells*. https://doi.org/10.1182/blood.2019003782

Qi, F., Meng, Q., Hayashi, I., & Kobayashi, J. (2020). FXR1 is a novel MRE11-binding partner and participates in oxidative stress responses. *Journal of Radiation Research*, *61*(3), 368–375. https://doi.org/10.1093/jrr/rraa011

Rickman, K., & Smogorzewska, A. (2019). Advances in understanding DNA processing

and protection at stalled replication forks. *Journal of Cell Biology*, *218*(4), 1096–1107. https://doi.org/10.1083/jcb.201809012

Saldivar, J. C., Cortez, D., & Cimprich, K. A. (2017). The essential kinase ATR: Ensuring faithful duplication of a challenging genome. *Nature Reviews Molecular Cell Biology*, *18*(10), 622–636. https://doi.org/10.1038/nrm.2017.67

Schwarz, D. A., Katayama, C. D., & Hedrick, S. M. (1998). Schlafen, a new family of growth regulatory genes that affect thymocyte development. *Immunity*, *9*(5), 657–668. https://doi.org/10.1016/S1074-7613(00)80663-9

Sousa, F. G., Matuo, R., Tang, S. W., Rajapakse, V. N., Luna, A., Sander, C., Varma, S., Simon, P. H. G., Doroshow, J. H., Reinhold, W. C., & Pommier, Y. (2015). Alterations of DNA repair genes in the NCI-60 cell lines and their predictive value for anticancer drug activity. *DNA Repair*, *28*, 107–115. https://doi.org/10.1016/j.dnarep.2015.01.011

Yang, J. Y., Deng, X. Y., Li, Y. S., Ma, X. C., Feng, J. X., Yu, B., Chen, Y., Luo, Y. L., Wang, X., Chen, M. L., Fang, Z. X., Zheng, F. X., Li, Y. P., Zhong, Q., Kang, T. B., Song, L. B., Xu, R. H., Zeng, M. S., Chen, W., … Gao, S. (2018). Structure of Schlafen13 reveals a new class of tRNA/rRNA- targeting RNase engaged in translational control. *Nature Communications*, *9*(1). https://doi.org/10.1038/s41467-

018-03544-x

Zhang, B., Ramkumar, K., Cardnell, R. J., Gay, C. M., Stewart, C. A., Wang, W. L., Fujimoto, J., Wistuba, I. I., & Byers, L. A. (2021). A wake-up call for cancer DNA damage: the role of Schlafen 11 (SLFN11) across multiple cancers. In *British Journal of Cancer* (Vol. 125, Issue 10, pp. 1333–1340). Springer Nature. https://doi.org/10.1038/s41416-021-01476-w

Zoppoli, G., Regairaz, M., Leo, E., Reinhold, W. C., Varma, S., Ballestrero, A., Doroshow, J. H., & Pommier, Y. (2012). Putative DNA/RNA helicase Schlafen-11 (SLFN11) sensitizes cancer cells to DNA-damaging agents. *Proceedings of the National Academy of Sciences of the United States of America*, *109*(37), 15030–15035. https://doi.org/10.1073/pnas.1205943109

Figure legends

Figure 1. Expression of SLFN11 with a mutated ribonuclease domain sensitizes cells to treatment with HU.

(A) Multiple sequence alignments of the proposed active site regions of selected Schlafen proteins. The critical catalytic residues are indicated with E/D = *, K/R = o. The method used for alignment was MAFFT program (Genetyx-Mac). The conserved regions were from the Pfam database. (**B**) A schematic diagram of SLFN11 protein structure. Positions of the mutation in the ribonuclease domain are shown. **(C)** Western blots (WB) analysis of DOX-induced expression of SLFN11. HAP1 *SLFN11*$^{-/-}$ cells were transduced with wild-type SLFN11 or the ribonuclease mutant SLFN11. Lentivirally transduced cells were treated with 2 μg/ml doxycycline (DOX) for 48 h for expression. **(D)** Cell proliferation profile of *SLFN11*$^{-/-}$ HAP1 cells with indicated transgenes. (**E**) Cell survival assay of HAP1 cells with indicated genotypes treated with indicated doses of hydroxyurea (HU) for 72 h. Data represent mean ± SD.

Figure 2. Expression of SLFN11 with a mutated ribonuclease domain accelerates the degradation of stalled replication forks.

(A) A schema of the experimental protocol (upper). Quantification results of fork degradation in HAP1 cells with the indicated genotypes in the presence of HU (Below). The CldU tract length of over 300 DNA fibers were measured in each sample. To minimize the effects of observer bias, the images were captured and analyzed in a blinded manner. P values were calculated by one-way ANOVA with Tukey's multiple-comparisons test. Mean ± SD are shown. n.s., not significant. ****, $p<0.0001$. **(B)** Representative DNA fiber images of HAP1 cells with indicated genotypes.

Figure 3. Expression of SLFN11 with a mutated ribonuclease domain prevents RPA and RAD51 recruitment to DNA damage sites

Quantification and representative images of RAD51 **(A)** and RPA **(B)** foci per cell in HAP1 cell derivative with the indicated genotypes. FLAG-tagged wild-type and RNase mutant SLFN11 re-expression *SLFN11*$^{-/-}$ cells were pre-treated with 2 μg/ml doxycycline (DOX) for 48 h for expression. Each dot represents the number of foci per nucleus in a single cell. Cells were exposed to 4 mM HU for 5 h and stained with the indicated antibodies. Mean ± SEM ($n \geqslant 500$) are shown for each condition. The P values were calculated using one-way ANOVA with Tukey's multiple-comparisons test. Representative images are shown. ***: $p=0.0002$. ****: $p<0.0001$

Figure 4. DNA2 and MRE11 nucleases, but not FXR1, are responsible for cleavage of nascent DNA tracts.

(**A**) DNA2 (left), MRE11 (middle) or FXR1 (right) depletion by siRNA in the wild-type and *SLFN11*$^{-/-}$ HAP1 cells was confirmed by western blotting analysis. Cells were collected 72 h after transfection with siRNA. Asterisks (*) represents a non-specific band. **(B)** DNA fiber assay results in HAP1 cells. A schema of DNA fiber assay protocol (upper) is shown. Cells were treated with luciferase negative control (siLuc) or siRNA targeting DNA2, MRE11 or FXR1 for 24 h before DOX-induced expression of wild-type SLFN11 or RNase mutant SLFN11, then exposed to 4 mM HU for 5 h. The length of more than 300 fibers were measured in each sample. P values were calculated by one-way ANOVA with Tukey's multiple-comparisons test. Mean ± SD are shown. n.s., not significant. ****, $p<0.0001$.

Figure 5. Expression of SLFN11 has no impact on ATR kinase levels in response to HU.

(A) The mRNA expression of ATR in HAP1 wild-type and *SLFN11*$^{-/-}$ cells complemented with wild-type or RNase mutant SLFN11 after 4 mM HU treatment for 5 h were analyzed by reverse transcription-PCR (RT-PCR). **(B)** HAP1 cells with indicated genotypes were

treated with 4 mM of HU for 5 h. Then, the cells were harvested and analyzed by western blotting using the indicated antibodies.


A
hSLFN11 201 YGEILPFPESQLVEFKQFSTKHFQEYVKRTIPEYVPAFANTGGGYLFIGVDDKSREVL 258
hSLFN5 191 YLEKLNLPESTHVEFVMFSTD-VSHCVKDRLPKCVSAFANTEGGYVFFGVHDETCQVI 239
hSLFN13 207 YGEILSFPESPSIEFKQFSTKHIQQYVENIIPEYISAFANTEGGYLFIGVDDKSRKVL 257
mSLFN8 204 YGQCLLFSESTSIEFKQFSTKHVQAYMKNIIPEYISAFANTQGGYLFIGVDDKRI-IL 254
mSLFN9 204 YGQRLLFSESTSIEFKQFDTENAQKYMKDIIPEYISAFANTQGGYLFIGVDDKSI-IL 254
rSLFN13 204 YGQRLPFSESASIEFKQFSTRRAHEYIKSVIPEYISAFANTQGGYLLFGVDDESKRVL 254

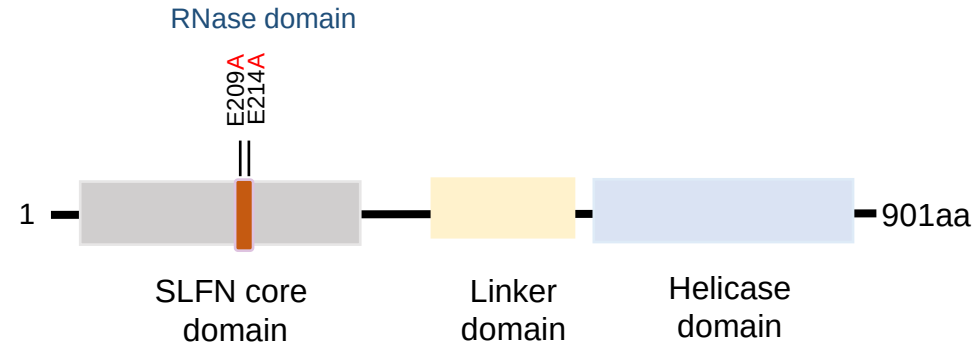
B
Full length of hSLFN11
RNase domain
E209A
E214A
1
901aa
SLFN core domain
Linker domain
Helicase domain

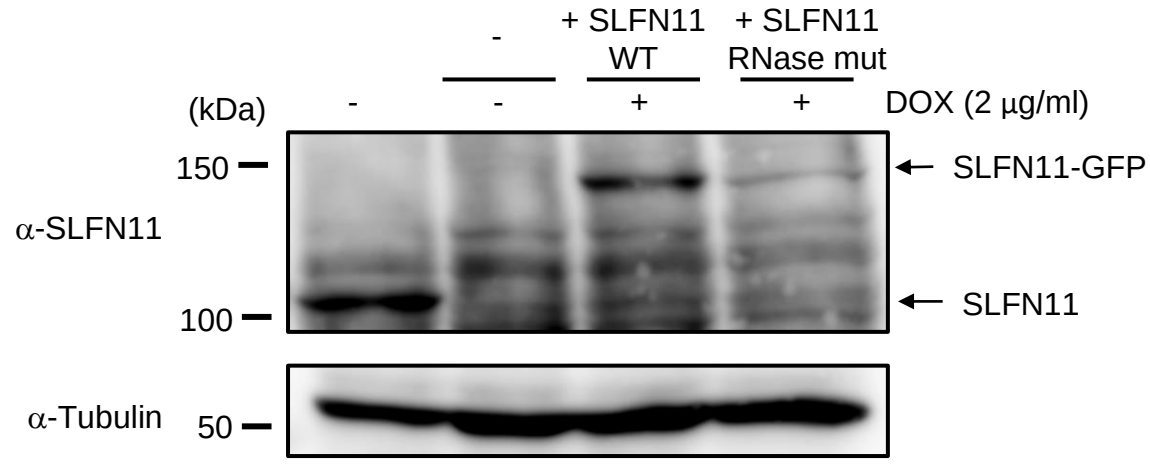
C
HAP1
WT
SLFN11-/-
+ SLFN11 WT
+ SLFN11 RNase mut
(kDa)
DOX (2 μg/ml)
150
100
α-SLFN11
SLFN11-GFP
SLFN11
α-Tubulin
50

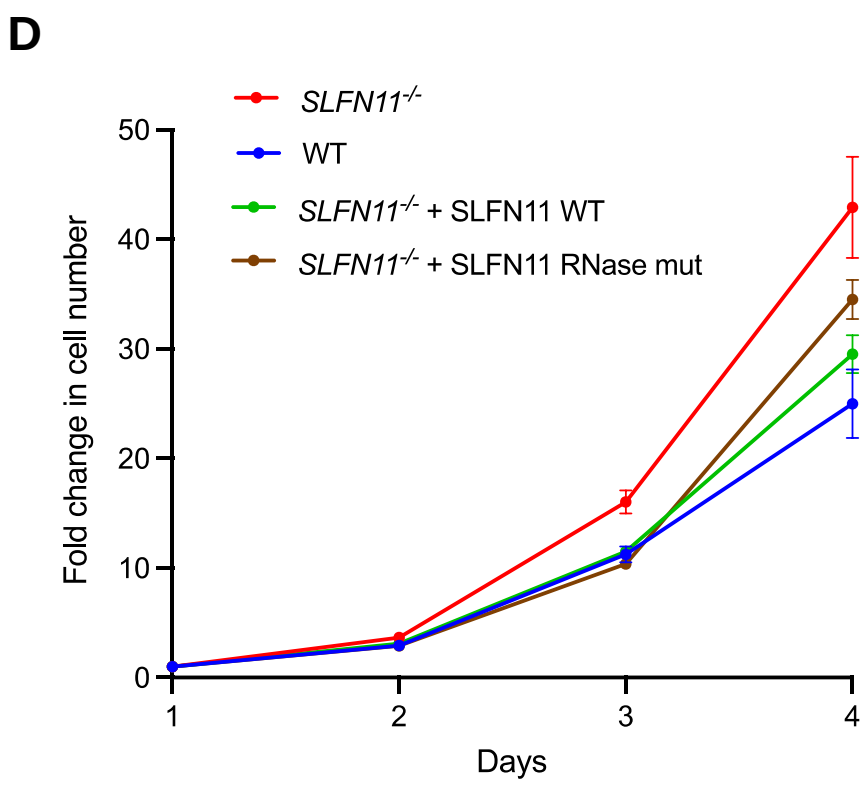
D
SLFN11-/-
WT
SLFN11-/- + SLFN11 WT
SLFN11-/- + SLFN11 RNase mut
Fold change in cell number
Days

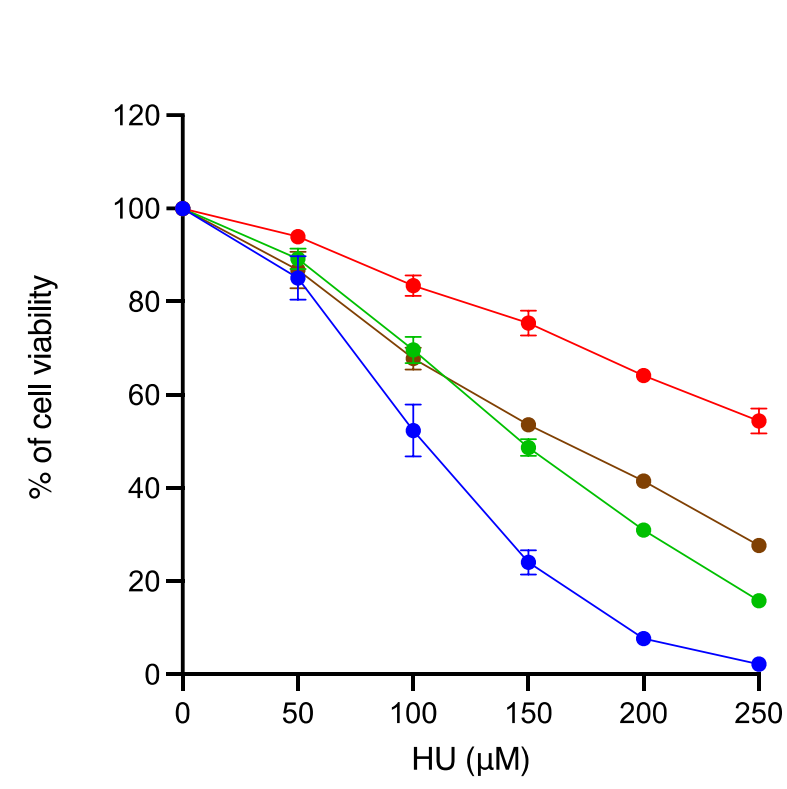
E
% of cell viability
HU (μM)

Figure 1

A

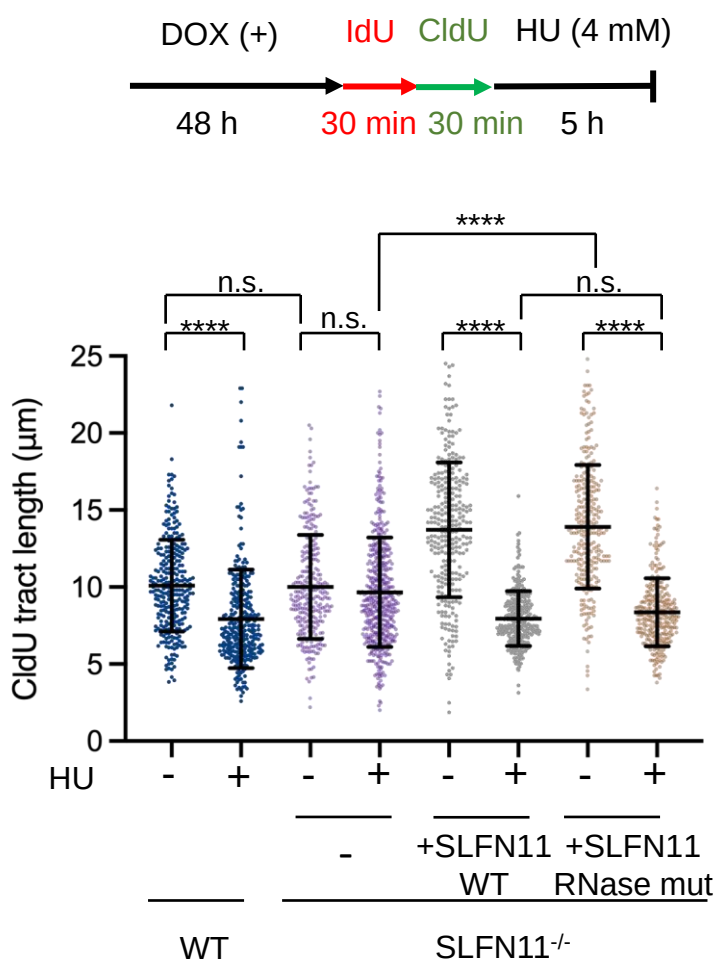
DOX (+)
IdU
CldU
HU (4 mM)
48 h
30 min
30 min
5 h
CldU tract length (μm)
25
20
15
10
5
0
****
n.s.
n.s.
****
n.s.
****
****
HU
-
+
-
+
-
+
-
+
-
+SLFN11 WT
+SLFN11 RNase mut
WT
SLFN11-/-

B

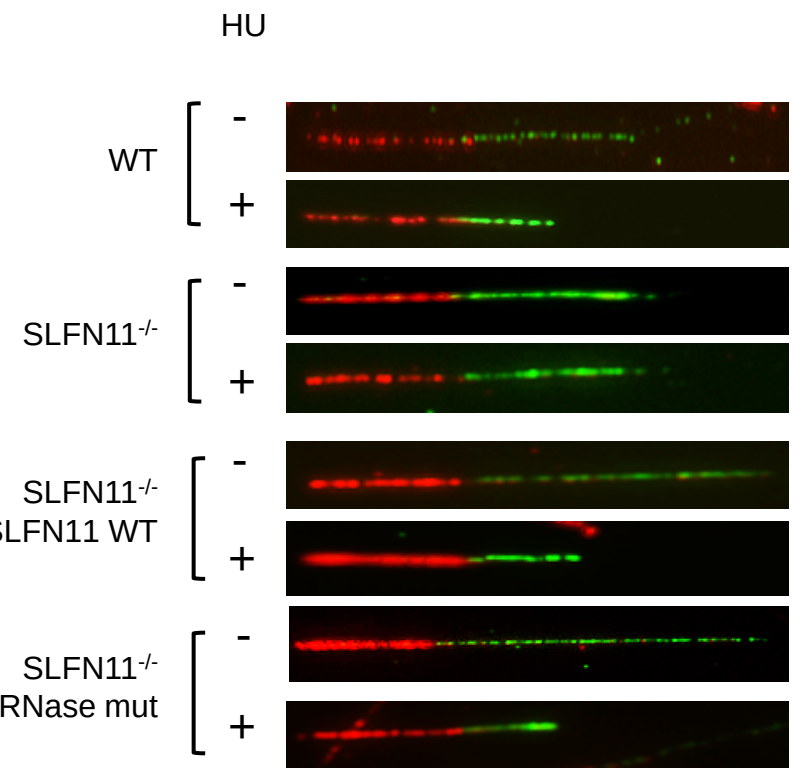
HU
WT
-
+
SLFN11-/-
-
+
SLFN11-/-
+ SLFN11 WT
-
+
SLFN11-/-
+SLFN11 RNase mut
-
+

Figure 2

A

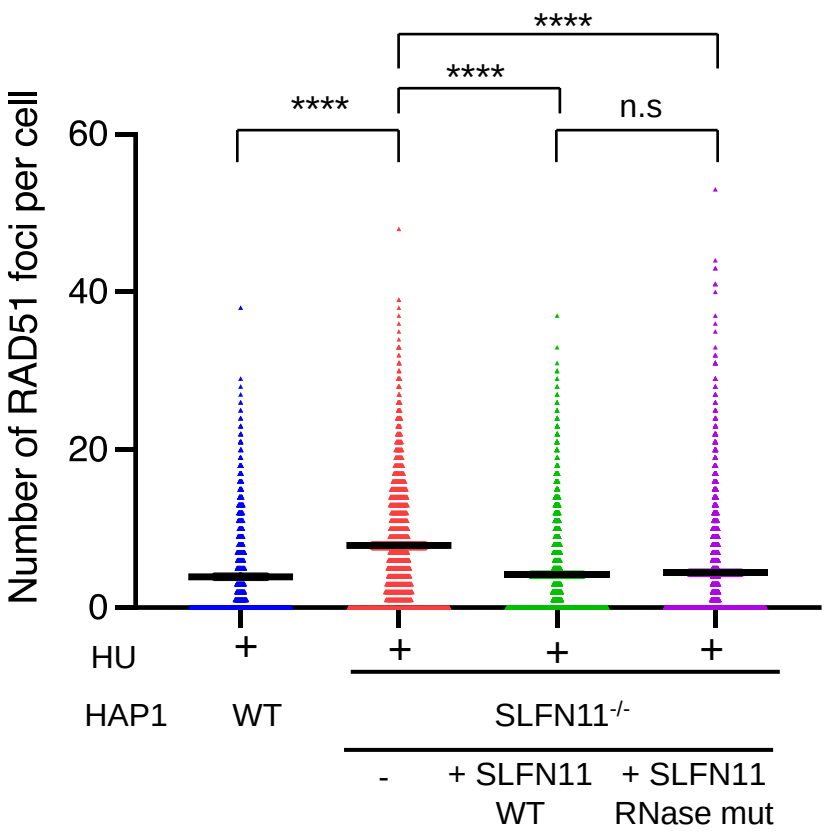
Number of RAD51 foci per cell
60
40
20
0
****
****
****
n.s
HU
+
+
+
+
HAP1
WT
SLFN11-/-
-
+ SLFN11 WT
+ SLFN11 RNase mut

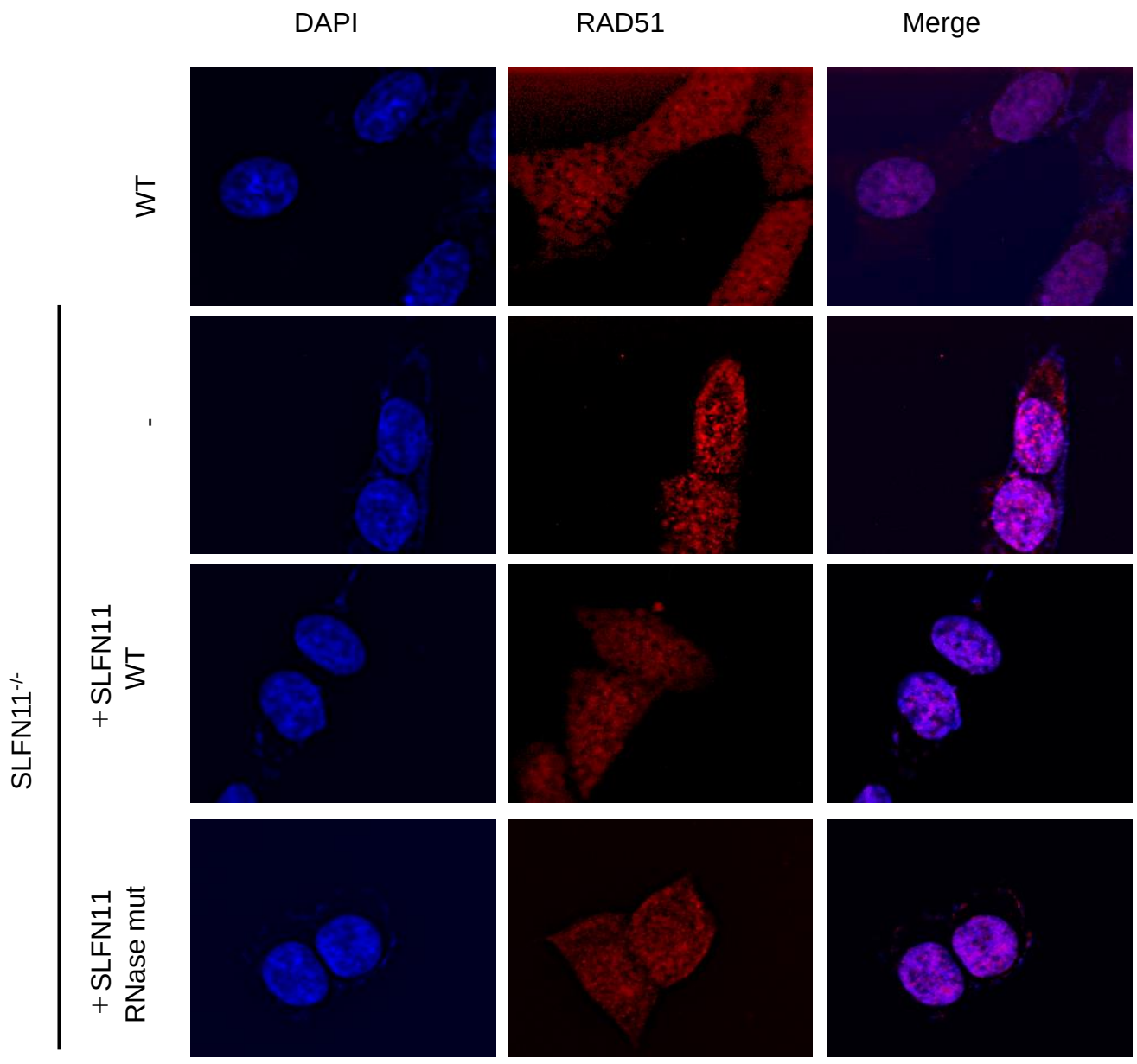
DAPI
RAD51
Merge
WT
-
+ SLFN11 WT
+ SLFN11 RNase mut
SLFN11-/-

B

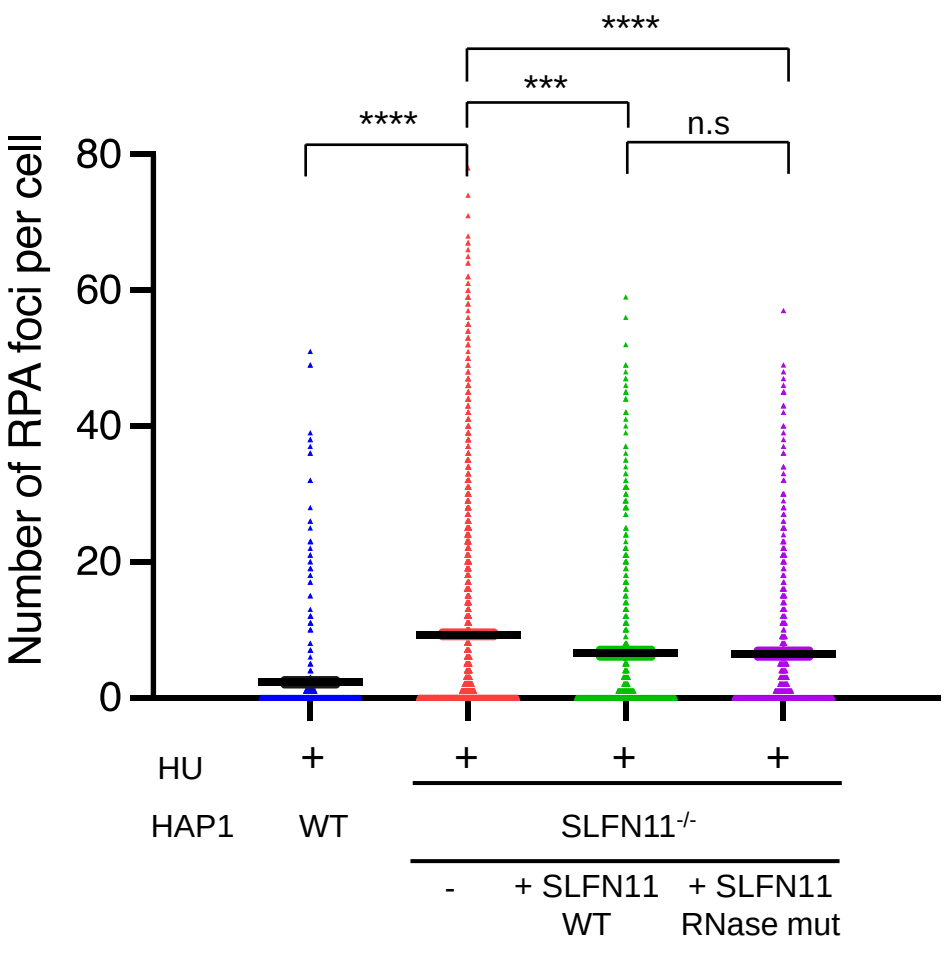
Number of RPA foci per cell
80
60
40
20
0
****
***
n.s
HU
+
+
+
+
HAP1
WT
SLFN11-/-
-
+ SLFN11 WT
+ SLFN11 RNase mut

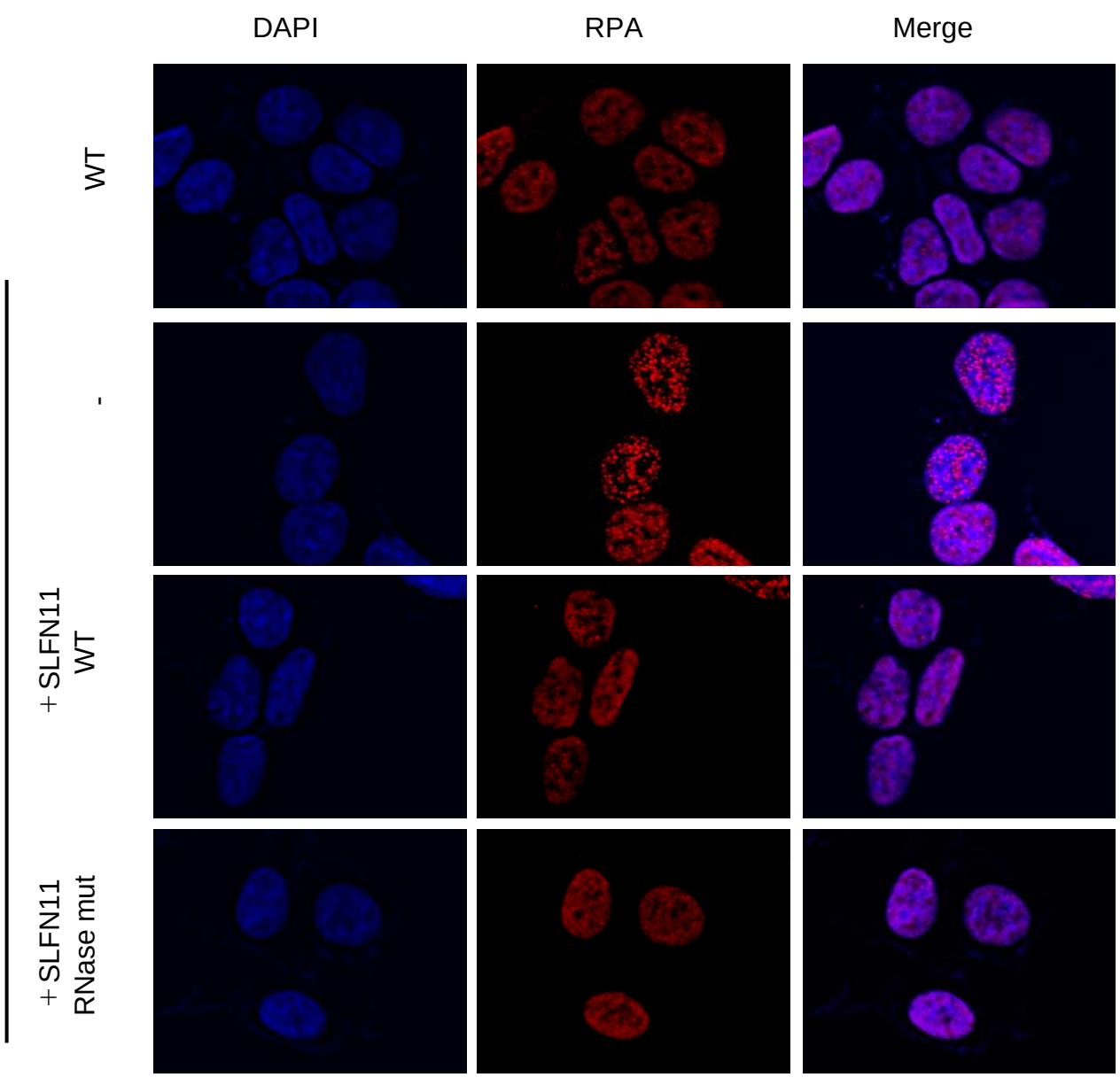
DAPI
RPA
Merge
WT
-
+ SLFN11 WT
+ SLFN11 RNase mut
SLFN11-/-

Figure 3

A

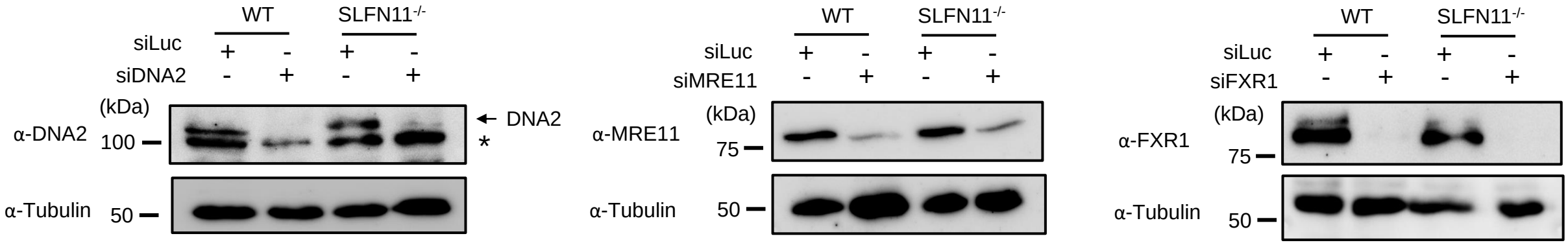
WT
SLFN11-/-
siLuc + - + -
siDNA2 - + - +
(kDa)
α-DNA2
100
DNA2
*
α-Tubulin
50
WT
SLFN11-/-
siLuc + - + -
siMRE11 - + - +
(kDa)
α-MRE11
75
α-Tubulin
50
WT
SLFN11-/-
siLuc + - + -
siFXR1 - + - +
(kDa)
α-FXR1
75
α-Tubulin
50

B

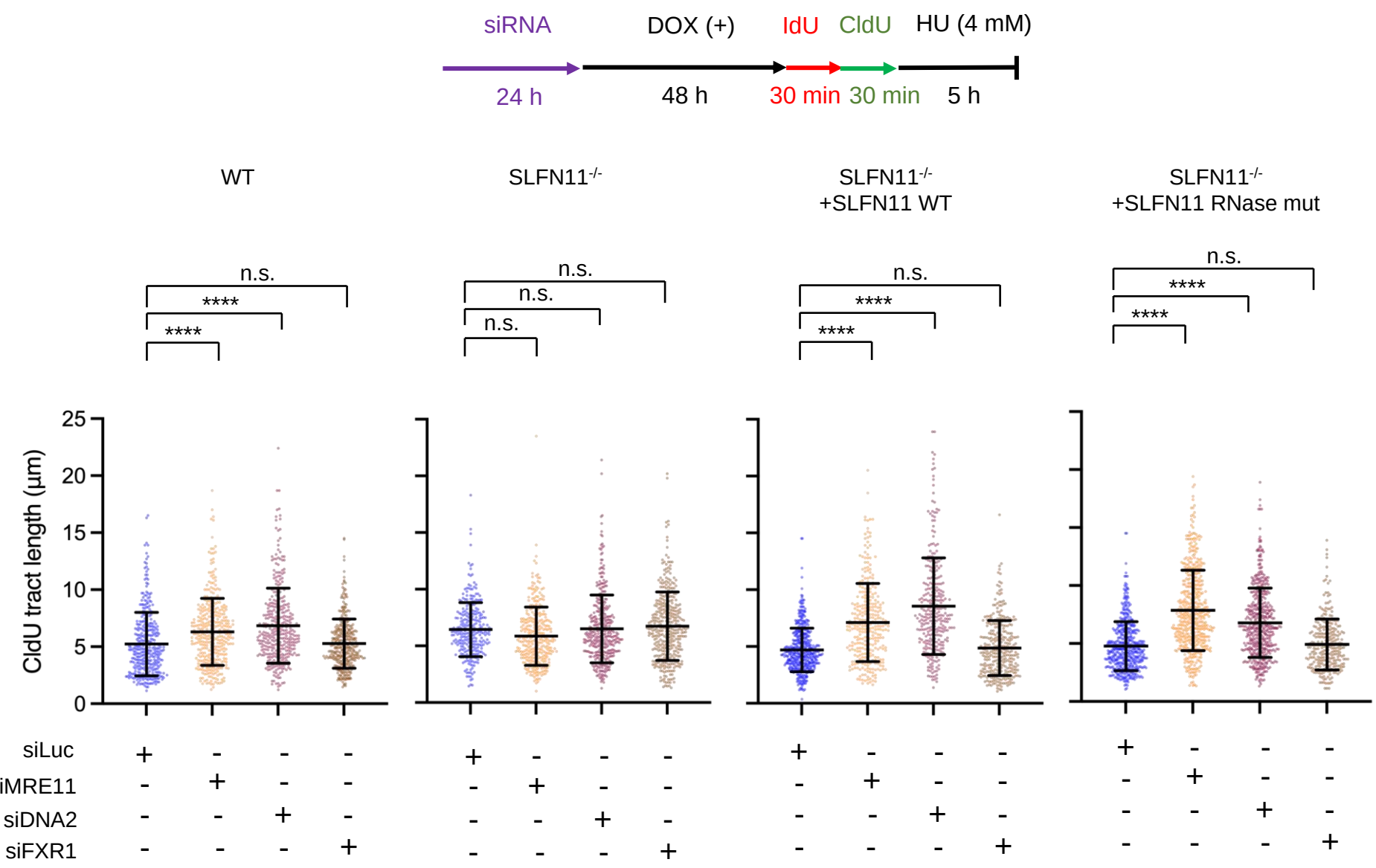
siRNA
DOX (+)
IdU
CldU
HU (4 mM)
24 h
48 h
30 min
30 min
5 h
WT
SLFN11-/-
SLFN11-/- +SLFN11 WT
SLFN11-/- +SLFN11 RNase mut
n.s.
****
CldU tract length (μm)
25
20
15
10
5
0
siLuc + - - - + - - - + - - - + - - -
siMRE11 - + - - - + - - - + - - - + - -
siDNA2 - - + - - - + - - - + - - - + -
siFXR1 - - - + - - - + - - - + - - - +

Figure 4

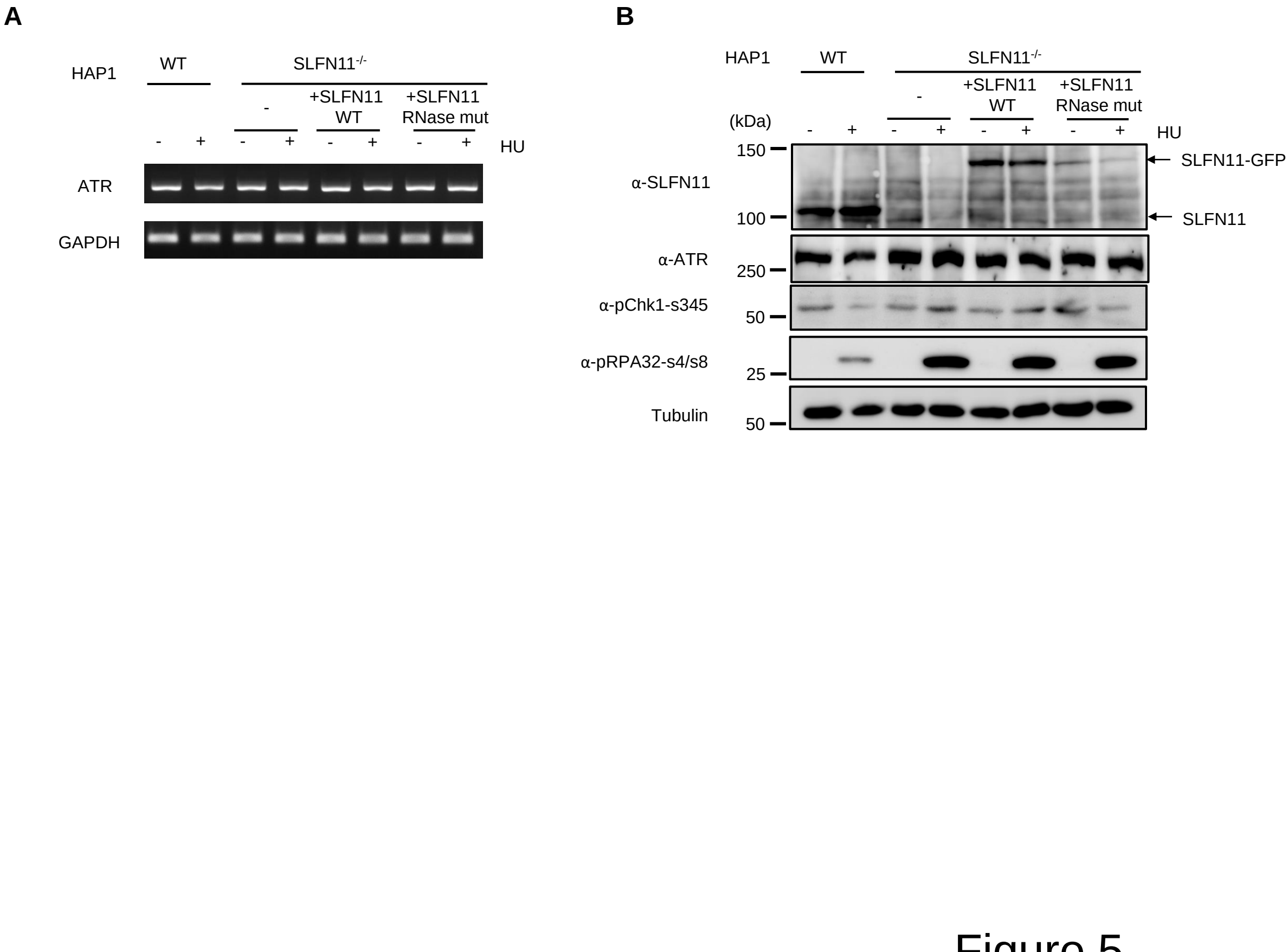
A
HAP1
WT
SLFN11-/-
-
+SLFN11 WT
+SLFN11 RNase mut
- + - + - + - +
HU
ATR
GAPDH
B
HAP1
WT
SLFN11-/-
-
+SLFN11 WT
+SLFN11 RNase mut
(kDa)
- + - + - + - +
HU
150
100
250
50
25
50
α-SLFN11
α-ATR
α-pChk1-s345
α-pRPA32-s4/s8
Tubulin
SLFN11-GFP
SLFN11

Figure 5

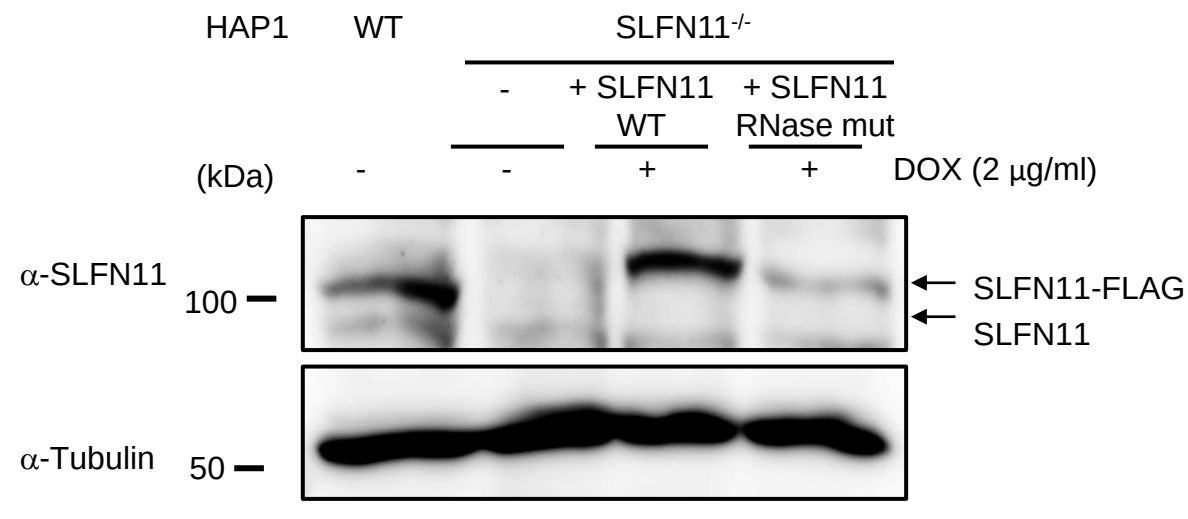

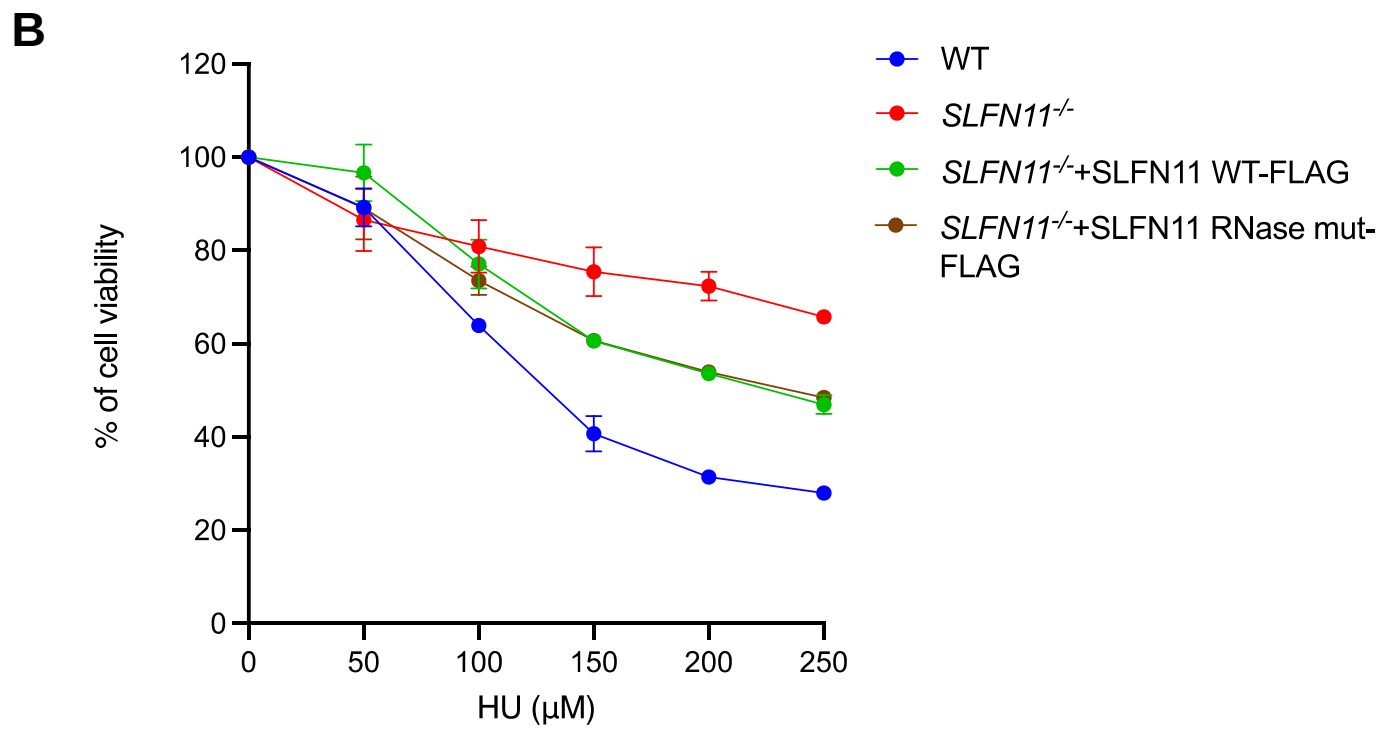

Supplementary figure 1

Supplementary figure 1. Expression of SLFN11 with a FLAG-tagged ribonuclease mutant domain sensitizes cells to treatment with HU.
(A) Western blots (WB) analysis of DOX-induced expression of SLFN11. HAP1 *SLFN11*$^{-/-}$ cells were transduced with FLAG-tagged wild-type SLFN11 or the RNase mutant SLFN11. Lentivirally transduced cells were treated with 2 μg/ml doxycycline (DOX) for 48 h for expression. (**B**) Cell survival assay of HAP1 cells with indicated genotypes treated with indicated doses of hydroxyurea (HU) for 72 h. Data represent mean ± SD.

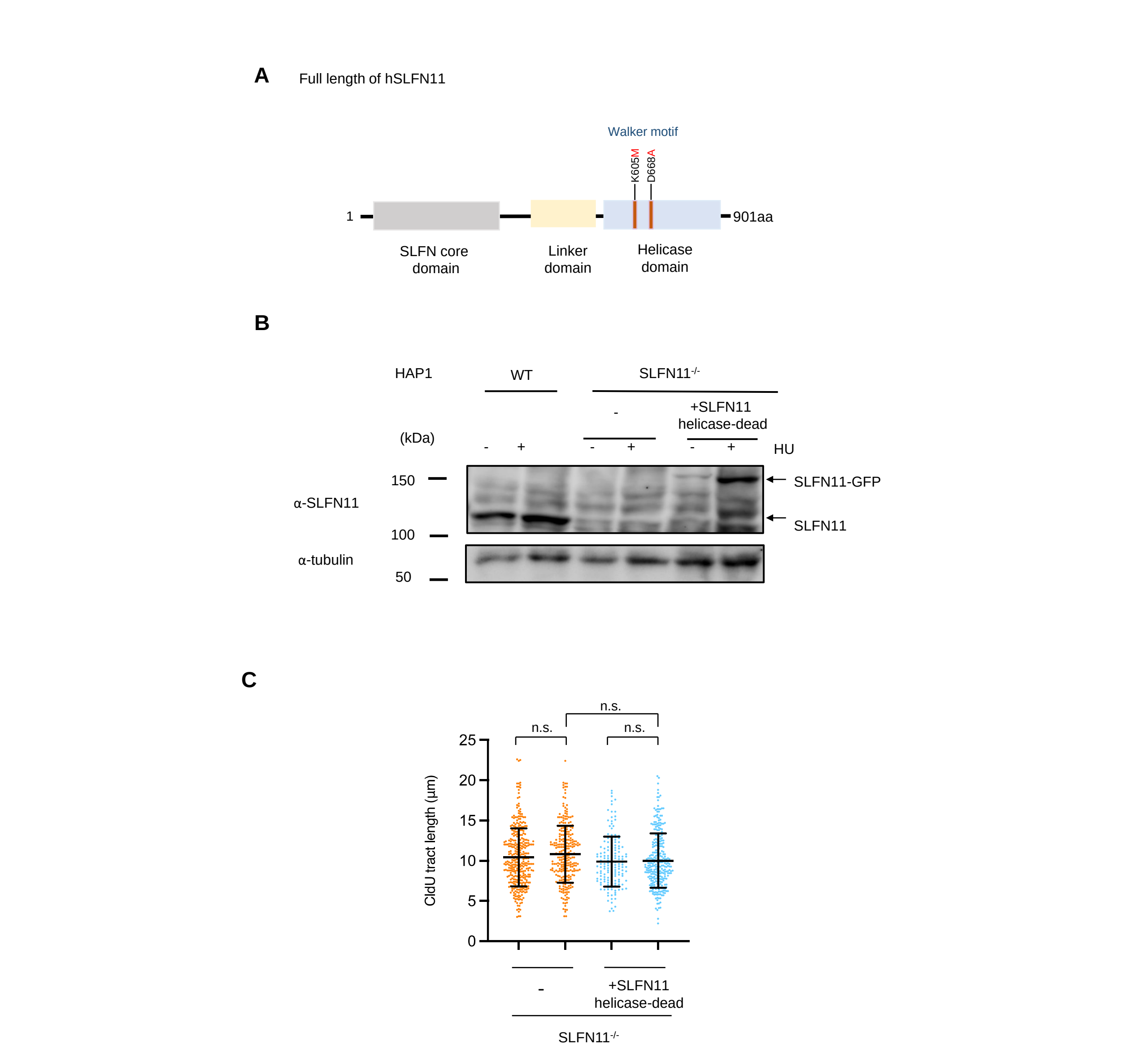

Supplementary Figure 2

Supplementary Figure 2. Expression of *SLFN11* with a mutated helicase domain didn't accelerate the degradation of stalled replication forks.

(A) A schematic diagram of SLFN11 protein structure. Positions of the mutation in the ATPase domain are shown. **(B)** Western blots (WB) analysis of DOX-induced expression of SLFN11s. HAP1 *SLFN11*$^{-/-}$ cells were transduced with an ATPase domain mutant SLFN11. **(C)** Quantification results of fork degradation in HAP1 cells with the indicated genotypes in the presence of HU. The CldU tract length of over 300 DNA fibers were measured in each sample. To minimize the effects of observer bias, the images were captured and analyzed in a blinded manner. P values were calculated by one-way ANOVA with Tukey's multiple-comparisons test. Mean ± SD are shown. n.s., not significant. ****, $p<0.0001$.

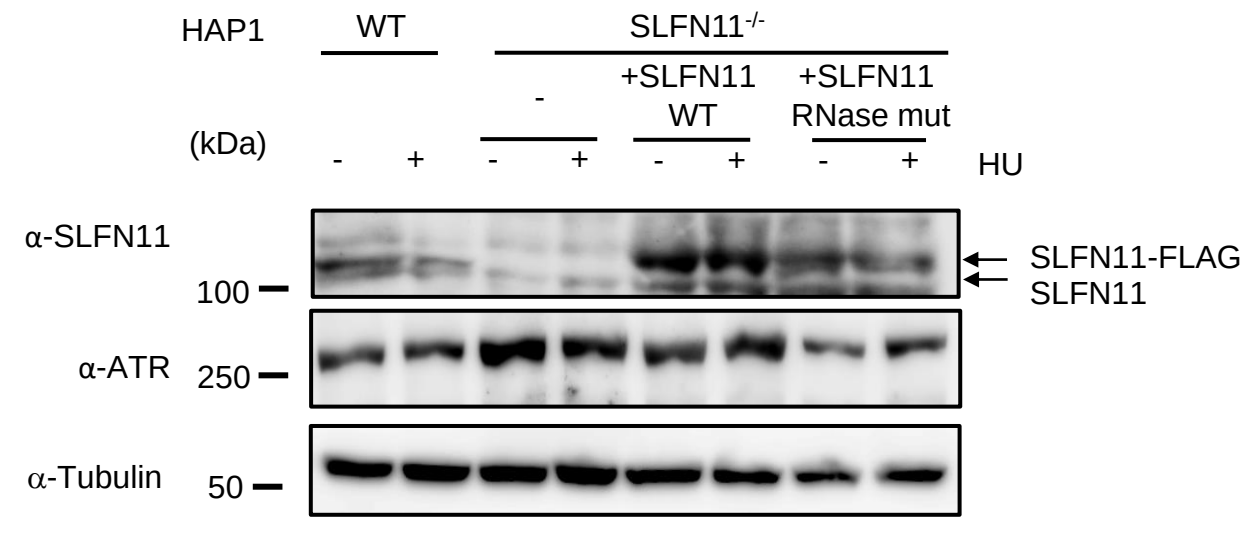

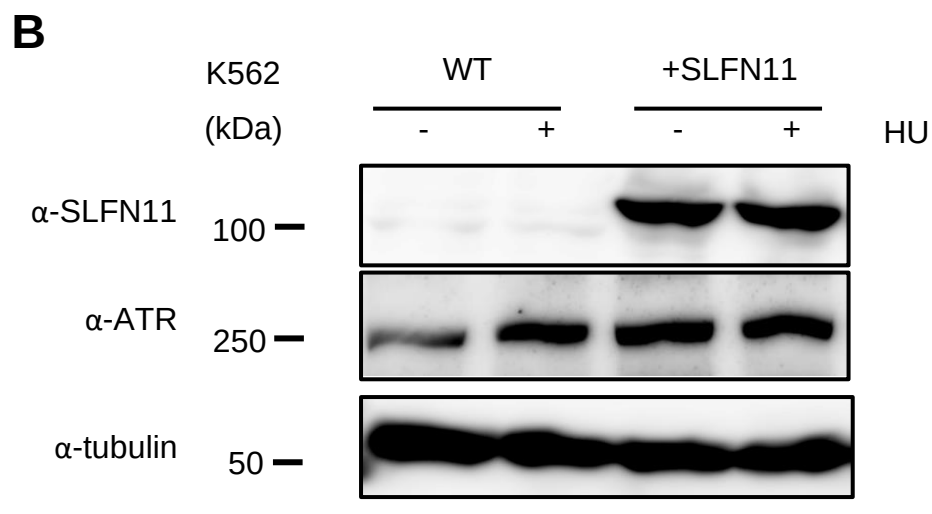

Supplementary figure 3

Supplementary figure 3. Expression of RNase mutant SLFN11 has no effect on ATR protein levels in response to HU.

(A) FLAG-tagged wild-type and RNase mutant SLFN11 were transfected in *SLFN11*$^{-/-}$ HAP1 cells, and pre-treated with 2 μg/ml doxycycline (DOX) for 48 h for expression. HAP1 cells with indicated genotypes were treated with 4 mM of HU for 5 h. Then, the cells were harvested and analyzed by western blotting using the indicated antibodies. **(B)** Western blot (WB) analysis of wild-type and *SLFN11*$^{-/-}$ K562 cells. K562 cells with indicated genotypes were treated with 4 mM of HU for 5 h.